Natural Hazards (2022) 110:2059–2086
https://doi.org/10.1007/s11069-021-05025-9

ORIGINAL PAPER

Economic damages due to extreme precipitation during tropical storms: evidence from Jamaica

Dino Collalti[1] · Eric Strobl[1]

Received: 11 April 2021 / Accepted: 5 September 2021 / Published online: 20 September 2021

Abstract
This study investigates economic damage risk due to extreme rainfall during tropical storms in Jamaica. To this end, remote sensing precipitation data are linked to regional damage data for five storms. Extreme value modelling of precipitation is combined with an estimated damage function and satellite-derived nightlight intensity to estimate local risk in monetary terms. The results show that variation in maximum rainfall during a storm significantly contributes to parish level damages even after controlling for local wind speed. For instance, the damage risk for a 20 year rainfall event in Jamaica is estimated to be at least 238 million USD, i.e. about 1.5% of Jamaica's yearly GDP.

Keywords Tropical cyclones · Extreme events · Rainfall

1 Introduction

Tropical cyclones (TCs) are among the most destructive natural disasters, estimated to have caused over 800 USD billion in damages globally over the last 20 years.[1] Damages attributable to these storms are mainly due to three factors, namely extreme wind, storm surge, and torrential rainfall (Bakkensen et al. 2018; Park et al. 2013; Lin et al. 2010). The literature modelling the economic impact has, however, mainly focused on damages as a result of wind, and to a lesser extent storm surge (Emanuel 2005; Nordhaus 2006; Hu et al. 2016; Baradaranshoraka et al. 2017; Masoomi et al. 2019; Hatzikyriakou and Lin 2018; Do et al. 2020), due to the difficulties associated with large-scale flood modelling as a result of extreme precipitation (Murnane and Elsner 2012; Zhai and Jiang 2014). This is often justified on the grounds that wind is strongly correlated with rainfall during a TC and thus that wind exposure will capture damages due to rainfall as well. However, recent evidence suggests that rainfall is not absolutely dependant on TC intensity, "*...suggesting that stronger TCs do not have systematically higher maximum rain rates than weaker storms*." (Yu et al.

[1] Authors' own calculation using EMDAT database.

✉ Dino Collalti
dino.collalti@windowslive.com

[1] Department of Economics and Oeschger Center for Climate Change Research, University of Bern, Bern, Switzerland

2017). It has also been shown that the positive correlation between wind speed and rainfall may only be true over the ocean and not on land (Jiang et al. 2008).

The failure to take account of extreme precipitation in damage estimation arguably neglects an important driver of the economic costs due to TCs (Czajkowski et al. 2011; Rezapour and Baldock 2014; Rappaport 2014; Park et al. 2015; Bakkensen et al. 2018). For instance, available data for the Caribbean suggest that rainfall is either the primary or secondary cause of damages in 75% of TC events.[2] While the influence of anthropogenic climate change on TC frequency, general intensity, and affected areas is still a matter of debate, there is a general consensus that rainfall-heavy TCs will likely become more frequent in the future (Emanuel 2013; Knutson et al. 2019; Van Oldenborgh et al. 2017; Villarini et al. 2014b; Grossmann and Morgan 2011; Walsh et al. 2016). Nevertheless, the link between extreme rainfall and economic damages is not well understood yet (Villarini et al. 2014a; Rosenzweig et al. 2018; Rözer et al. 2019). While non-hazard measures such as risk awareness, building type, and topography are important aspects, the most influential determinants for whether a building is damaged by flooding are local water depth and accumulated rainfall (Spekkers et al. 2013; Van Ootegem et al. 2015, 2018; Rözer et al. 2019). At the same time, short duration and high-intensity rainfall has been shown to be a major factor for the occurrence of landslides (Dou et al. 2019). Case studies have demonstrated that hazard scales that include rainfall in addition to wind speed are able to better predict the cost of TCs (Rezapour and Baldock 2014) and that wind only damage functions systematically underestimate damages by rainfall heavy typhoons in the Philippines (Eberenz et al. 2021).

The current study explicitly focuses on estimating the damage and risk associated with extreme precipitation during TCs, using Jamaica as a case study. Jamaica is arguably a particularly interesting setting for this purpose since the island is frequently afflicted by TCs. Excess rainfall is a major cause of destruction by inducing flash floods and landslides (Laing 2004). Moreover, due to the absence of large rivers, the volcanic origin of many hill-slopes, such floods and landslides, is common throughout most of the island (Miller et al. 2009). This allows the exploitation of spatial variation in rainfall intensity during TCs for the estimation of a rainfall-based damage function.

Importantly, the Planning Institute of Jamaica (PIOJ) has compiled consistent and detailed damage reports for most storms since the turn of the century. The lack of consistently reported damages often introduces additional uncertainty gitepbakkensen2018impact. Here, reports for five major TCs over the period of 2001–2012 are used to construct parish level information on economic damages.[3] Given that excess rainfall damages during TCs are often due to short, high intensity events (Larsen and Simon 1993). These damage data are coupled with high resolution, high frequency remote sensing precipitation data from the Global Precipitation Measurement Mission (Huffman et al. 2015a; Hou et al. 2014). Remote sensing information like the Tropical Rainfall Measuring Mission (TRMM) has been used extensively for the monitoring of TCs (Lonfat et al. 2004; Chen et al. 2006; Lau et al. 2008; Hendricks et al. 2010; Jiang et al. 2011; Villarini et al. 2011; Hence and Houze Jr 2011; Matyas and Silva 2013).

Using our data, we estimate a precipitation-dependent damage function via regression analysis, while controlling for the maximum wind speed during the storm. We then employ

[2] Authors' own calculations using the EMDAT database on damages due to natural disasters.

[3] Parish is the main administrative regional breakdown of Jamaica.

the precipitation data to generate return level maps using an extreme value model in the spirit of Demirdjian et al. (2018). Such a statistical approach has been shown to model extreme rainfall risk well in several case studies (Sugahara et al. 2009; Beguería et al. 2011; Tramblay et al. 2013). In conjunction with the estimated damage function and a proxy of the economic activity distribution derived from remote sensing nightlight intensity, information on the severity of a rainfall event occurring with a certain probability yields risk maps of economic damages due to extreme rainfall for Jamaica. The outlined method does not rely on large-scale hydrological models and should easily extend to other regions where gauge-based precipitation data are scarce.

The remainder of the paper is organized as follows: Sect. 2 presents the study region and describes the data. Section 3 details the methodology. Section 4 presents results while Sect. 5 discusses the findings. Finally, Sect. 6 concludes.

2 Study region and data

2.1 Study region

Jamaica is an island country situated in the Caribbean and is the third-largest island of the Greater Antilles after Cuba and Hispaniola. With a population of 2.9 Mio. (World Bank Group 2020), Jamaica is one of the larger states in the region and is ranked as a high development country by the UN human development index (Conceição 2019). Jamaica consists of 14 parishes, which is the highest regional administrative unit for the island. The country's economy is mixed but increasingly based on tourism and finance, while the export of agricultural commodities is declining (Johnston and Montecino 2012). Jamaica has two major cities, the capital Kingston in the south-east and Montego Bay in the north-west, known for its tourism. The islands geography is dominated by its central high plains and mountains. The Blue Mountains in the east, famous for their coffee plantations, constitutes Jamaica's highest point at 2.256 m. Jamaica is highly exposed to natural disasters such as TCs, earthquakes and droughts (Carby 2018). Between 1988 and 2012, 11 named storms made landfall in Jamaica and caused severe destruction (The World Bank Group 2018). The climate in Jamaica is tropical with little seasonality in temperature. However, due to the north-east trade winds, the period from November to March is dry and the rainy season lasts from April to October. Highest rainfall on the island occurs in the east, the north-eastern coast averaging more than 400 mm a year. Near the peak of the Blue Mountains, the average is more than 625 mm a year (Nkemdirim 1979). Summary of the data of Jamaica subsequently presented is given in Table 1.

2.2 Damages

The Planning Institute of Jamaica (PIOJ) has produced consistent socio-economic damage reports after damaging tropical storms since Hurricane Michelle in October 2001. In this regard, the PIOJ follows the United Nations Economic Commission for Latin America and the Caribbean (UNECLAC) Damage and Loss Assessment (DaLA) methodology (Bradshaw 2003). Each report contains a precise description of the event, preliminary rainfall reports, description of social trauma, emergency actions, and an assessment of economic damages. The assessment of economic damages considers damages in terms of three 'sectors,' namely agriculture (crop and livestock), public infrastructure (roads, schools and others), and housing.

Since not all reports provide this information at the parish level, the analysis in this study is restricted to events for which there is such a regional breakdown, i.e. five storms: Hurricane Michelle 2001, Hurricane Dean 2007, Hurricane Gustav 2008, Tropical Storm Nicole 2010 and Hurricane Sandy 2012. Additionally, even when there is regional information, in some reports, not all three of the main sectors are necessarily covered sub-nationally. Table 2 shows which sectoral damages have been reported by parish. When not all three sectors are covered sub-nationally, the damage measure was calculated as the proportion of damages with data at the parish level and scaled to total reported damages (including countrywide aggregates). For instance, during Hurricane Sandy in 2012, 25% ($3.7 M) of the damage to agriculture occurred in the parish of Portland and 30% (5,190) of all damaged houses were located there. Thus, it was assumed that Portland accounted for 27.5% or 29.4 M USD of the estimated total damage of 106.6 M USD across all three sectors. One should note that in most reports, the parish of Kingston is counted together with the parish of St. Andrew due to its small size and their proximity, leaving 13 distinct regions for the analysis. The per parish damages originally reported in USD are inflation adjusted with the Federal Reserve Economic Data (FRED) consumer price index (U.S. Bureau of Labor Statistics 2019, CPI), normalized to February 1st 2020 values. The data from the PIOJ reports for 13 Jamaican parishes and 5 TCs provide a total of 65 regional level damage observations.

2.3 Precipitation

The source for precipitation data is version 06B of the Global Precipitation Measurement (GPM) Integrated Multi-satellitE Retrievals (IMERG), a satellite based estimate (Huffman et al. 2015b). The satellite precipitation algorithm combines various microwave and infrared precipitation measurements to produce precipitation estimates, adjusted with surface gauge data. The resulting product is a half-hourly data set with near global coverage at a $0.1° \times 0.1°$ resolution for the sample period 01. June 2000-31. May 2019. The data have been pre-processed according to the accompanying tech-report (Huffman et al. 2020). One should note that the GPM's predecessor, the Tropical Rainfall Measuring Mission (Huffman et al. 2007, TRMM), has been regularly used in the context of extreme value modelling in meteorology (Furrer and Katz 2008; Demirdjian et al. 2018) and hydrology (Collischonn et al. 2008; Li et al. 2012).

2.4 Storm tracks

Information on the TCs in our analysis comes from the HURDAT Best Track Data (Landsea and Franklin 2013). The data provide six hourly observations on all tropical cyclones in the North Atlantic Basin, including the position of the eye and the maximum wind speed of the storm. Additional information on the spatial extent of the TCs is taken from the Extended Best Track Dataset (Demuth et al. 2006).

2.5 Nightlights

The economic exposure to extreme precipitation during a TC is unlikely to be evenly distributed even within a parish. Ideally, this should be taken into account when estimating a damage function using parish level damages. Given the lack of localized economic data from official statistical sources, nightlight intensity is often instead used as an alternative

Table 1 Data Summary

	Precipitation	Damages	Nightlight	Wind
Unit	mm/h	Mio. USD	–	km/h
Spatial	$0.1° \times 0.1°$	by parish	$30'' \times 30''$	$0.1° \times 0.1°$
Temporal	1/2-hourly	by storm	monthly	hourly
Source	GPM	PIOJ	DMSP/OLS	HURDAT
Maximum	120	63.31	63	268.54
Minimum	0	0.20	0	5.7
Mean	0.04	15.84	9.87	59.3
St. dev.	0.72	13.65	10.69	51.24

proxy (Chen and Nordhaus 2011; Elliott et al. 2015). To this end, gridded nightlight activity data from the Defense Meteorological Satellite Program (DMSP) Operational Linescan System (OLS) are used. The DMSP-OLS is available monthly at a high resolution of $30'' \times 30''$ (approx. 1 km × 1 km). Since the nightlight data are at a higher resolution than the GPM and damage data, the former is employed to aggregate the latter.[4]

3 Methodology

3.1 Framework

The risk of natural disasters consists of a combination of multiple factors (Peduzzi et al. 2012): the hazard itself (frequency and intensity), exposure (economic value, number of people) and vulnerability (the degree of loss given a hazard). Few attempts haven been made to incorporate extreme rainfall into the TC damage function. Li et al. (2019) define a precipitation intensity index analogue to the common used wind speed-based power dissipation index. However, they do not derive or validate this functional form. Bakkensen et al. (2018) utilizes the natural logarithm of maximum TC lifetime-rainfall of any weather station in a province, analogue to their use of the natural logarithm of maximum wind speed anywhere in the province. While both approaches highlight the importance of rainfall as a potential source of TC damages, they mimic their functional form of max. wind speed. Our approach is to first construct parish level wind and rainfall measures by TC, taking local exposure into account via the use of nightlight intensity measures. These measures are then combined with the parish level damage reports to estimate a precipitation specific damage function. The coefficient estimates and an extreme value analysis of precipitation are then combined to create spatial risk maps for Jamaica.

[4] For instance, the parish-level damage data require parish-level rainfall data. The GPM precipitation measurements do not naturally match the parish borders. Thus, the DMSP-OLS nightlight acts as intermediary in aggregating the GPM to the parish data.

Table 2 Overview of Parish Damage Data Availability

	Agricultural	Roadnetwork	Housing	Schools
Hurricane Michelle 2001	Yes	Yes		
Hurricane Dean 2007	Yes	Yes	Yes	Yes
Storm Gustav 2008	Yes	Yes	Yes	
Storm Nicole 2010	Yes	Yes	Yes	
Hurricane Sandy 2012	Yes		Yes	

3.2 Rainfall damage function

3.2.1 Windfield model

Following Strobl (2011) in calculating the local wind exposure during a storm, the Boose et al. (2004) version of the well-known Holland (1980) wind field model is utilized. The model estimates the location specific wind speed by taking into account the maximum sustained wind velocity anywhere in the storm, the forward path of the storm, the transition speed of the storm, the radius of maximum winds and the radial distance to the storm's eye. The model further adjusts for gust factor, surface friction, asymmetry due to the forward motion of the storm, and the shape of the wind profile curve. The source of storm data used is the HURDAT Best Track Data (Landsea and Franklin 2013). These 6-hourly track data are linearly interpolated to hourly observations. $WIND_{c,s,t}$, the wind experienced at any point c, during storm s at time t is given by:

$$WIND_{c,s,t} = GD\left[V_{m,s,t} - S\left(1 - \sin(T_{c,s,t})\right)\frac{V_{h,s,t}}{2}\right] \times \left[\left(\frac{R_{m,s,t}}{R_{c,s,t}}\right)^{B_{s,t}} \exp\left\{1 - \left[\frac{R_{m,s,t}}{R_{c,s,t}}\right]^{B_{s,t}}\right\}\right]^{1/2} \quad (1)$$

where $V_{m,s,t}$ is the maximum sustained wind velocity anywhere in the storm, $T_{c,s,t}$ is the clockwise angle between the forward path of the storm and a radial line from the storm centre to the c-th pixel of interest, $V_{h,s,t}$ is the forward velocity of the TC, $R_{m,s,t}$ is the radius of maximum winds, and $R_{c,s,t}$ is the radial distance from the centre of the storm to point c. The remaining ingredients in Eq. (1) consist of the gust factor G and the scaling parameters D for surface friction, S for the asymmetry due to the forward motion of the storm, and B for the shape of the wind profile curve. Points c are set equal to the centroid-coordinates of the GPM rainfall data and the storm-wise maximum wind speed for point c is given by $MWIND_{c,s}$. Appendix A.2 provides additional information on the model parameters.

3.2.2 Rainfall

Rainfall measures for the five storms are obtained for every GPM cell whose centroid is within the storm's reach at a certain observational time.[5] This is judged by comparing the radius of the outermost closed isobar provided by the Extended Best Track Dataset (Demuth et al. 2006) with the distance to the storm's eye. If the distance of a GPM cell's centroid to the storm's eye is smaller than the radius of the outermost closed isobar, that cell is currently affected by the storm. The Extended Best Track Dataset provides 6-hourly observations which we linearly interpolate to match the half-hourly GPM precipitation measurements. Then, all rainfall observations $RAIN_{c,s,t}$ can be summarized as the total rainfall $SRAIN_{c,s}$ or maximum rainfall during that storm, $MRAIN_{c,s}$. These two statistics are the extremes for describing the full distribution of $RAIN_{c,s,t}$.

3.2.3 Parish aggregation

The remote sensing information of rainfall, and thus, the calculated wind speed does not match the parish borders.[6] The monetary damages are, however, reported on the parish level. An intuitive way to aggregate rain and wind is to weight the cells by the share of nightlight activity in that cell relative to total parish nightlights. The grid of the nightlight activity is approx. 100× finer compared to the rainfall and wind speed grid. This allows one to down-weight cells that lie not entirely within a parish if weighted only by the within parish nightlight activity. It further controls for the value at risk of areas with more nightlight activity compared to areas that are unlit at night, e.g. large population centres. Cells are only added to the sum when their centroid lies within the parish. Specifically, j denotes a $30'' \times 30''$ nightlight activity cell and $w_{j,s}$ is the associated 3-month mean nightlight intensity prior to storm s and c is a $0.1° \times 0.1°$ rainfall or wind speed cell.[7] The nightlight weight is the fraction of the sum of nightlight activity in cell c that lies in parish i, divided by the total nightlight activity in parish i,

$$W_{c,s,i} = \frac{\sum_{j \in c | j \in i} w_{j,s}}{\sum_{j \in i} w_{j,s}}, \quad W_{c,s,i} \in (0,1). \tag{2}$$

With these weights, the gridded data can be aggregated to the parish level:

$$SRAIN_{i,s} = \sum_{c \in i} \left(SRAIN_{c,s} \times W_{c,s,i} \right), \tag{3}$$

$$MRAIN_{i,s} = \sum_{c \in i} \left(MRAIN_{c,s} \times W_{c,s,i} \right), \tag{4}$$

$$MWIND_{i,s} = \sum_{c \in i} \left(MWIND_{c,s} \times W_{c,s,i} \right), \tag{5}$$

[5] Even though many studies focus on landfalling TCs only, it has been shown that non-landfalling TCs can be equally destructive (López-Marrero and Castro-Rivera 2019).

[6] The data of rainfall and wind speed are on a $0.1° \times 0.1°$ grid.

[7] Note that, many nightlight cells j are in one rainfall (wind) cell c and many such cells c are in one parish i.

where $SRAIN_{i,s}$ and $MRAIN_{i,s}$ are the parish i, storm s total and maximum rainfall and $MWIND_{i,s}$ the respective maximum wind measure.

3.2.4 Damage function regression

The functional form which is assumed for the damage function has to be imposed in the regression. In this regard, it is well established that the destruction of TCs relates roughly to the cube of the maximum wind speed (Emanuel 2005). It is used as control for a tropical storms' power dissipation (Bertinelli and Strobl 2013). A priori, it is unclear whether maximum rainfall during a TC or the total rainfall adequately represents the effect of heavy rainfall during a TC. It follows that both measures should be included. Additionally, differences in parish economic endowment and thus potential damage is accounted for by including parish indicators. The linear regression is then given by

$$\begin{aligned} DAMAGES_{i,s} = \alpha + \beta_1 MRAIN_{i,s} + \beta_2 SRAIN_{i,s} \\ + \beta_3 MWIND^3{}_{i,s} + \gamma PARISH_i + \varepsilon_{i,s}. \end{aligned} \tag{6}$$

where $DAMAGES_{i,s}$ are the reported monetary damages, $MRAIN_{i,s}$ is the maximum hourly rainfall in a parish, $SRAIN_{i,s}$ is the sum of total rainfall, $MWIND^3{}_{i,s}$ is the cube of the maximum wind speed and $PARISH_i$ are indicator variables for parish i.[8] Potentially, other functional forms like polynomials or nonlinear models might provide a better fit to the data. Given the small sample size ($n = 65$), more evolved models could overfit.[9] Estimates obtained with an ordinary least squares regression of Eq. 6 are likely to generalize well and are interpretable.

We run several alternative specifications of Eq. 6. In Eq. 7, we use parish population POP_i measured by Jamaica's 2011 census to control for local economic endowment (Statistical Institute of Jamaica 2011) instead of parish indicators. This has the advantage of leaving more degrees of freedom for the model estimation. Robustness to outliers driving our results by omitting extreme observations as determined by Cook's distance (Cook 1977).[10] The data without outliers are then used to estimate Eq. 7.

$$\begin{aligned} DAMAGES_{i,s} = \alpha + \beta_1 MRAIN_{i,s} + \beta_3 MWIND^3{}_{i,s} \\ + \delta POP_i + \varepsilon_{i,s}. \end{aligned} \tag{7}$$

3.3 Extreme value modelling

The objective of a statistical extreme value analysis (EVA) is to quantify the tail behaviour of a process, for instance extreme rainfall occurring at a certain location. Such an EVA can be categorized into either a block maxima or a peaks-over-threshold approach. Both allow to fit a distribution to the extreme values of any sequence of i.i.d. random variables but differ in how they make use of the available information. The half-hourly time series X_i

[8] This corresponds to a parish fixed effects model. Inclusion of binary indicator variables results in group (parish) fixed means. This allows for heterogeneity in the mean damage of a parish for different storms.

[9] A model overfits if it captures residual variation (noise) that is not part of the data generating process. Such a model would not predict future observations reliably.

[10] We define a observation as outlier if it is 6× more influential than the average observation.

of rainfall in mm/h of GPM cell i with 333'072 observations from June 2000 to May 2019 are the subject of this EVA. Extreme rainfall in Jamaica happens often during TCs which occur 10–17 times in the Atlantic basin (NOAA 2019), not all affecting Jamaica. Due to this irregular pattern, a peak-over-threshold approach appropriately represents the physical phenomenon while making better use of the available information. The peaks-over-threshold approach is based on the Pickands-Balkema-de Haan theorem stating that threshold excesses $y = (X - u|X > u)$ have a corresponding generalized Pareto distribution (GPD) if the threshold u is sufficiently high (Coles et al. 2001, p. 75):

$$GPD(y) = \begin{cases} 1 - \left[1 + \xi\left(\frac{y}{\tilde{\sigma}}\right)\right]^{-\frac{1}{\xi}} & \text{for } \xi \neq 0, \\ 1 - \exp\left(-\frac{y}{\tilde{\sigma}}\right) & \text{for } \xi = 0, \end{cases} \tag{8}$$

where

$$\tilde{\sigma} = \sigma + \xi(u - \mu). \tag{9}$$

The parameters of the GPD distribution are location μ, scale σ and shape ξ. Here, a Poisson point-process (PPP) representation of threshold excesses is used, which allows one to a), directly estimate the likelihood function in terms of location μ, scale σ and shape ξ parameter, b) model non-stationarity in these parameters, and c) include the Poisson distributed threshold exceedance rate together with the threshold excesses in the inference. The EVA is carried out on the cell level by separately estimating $GPD(y_i)$ as in Eq. 8 where $y_i = (X_i - u_i|X_i > u_i)$ is the threshold excess of GPM cell i. The vector X_i contains the GPM rainfall measurements of cell i and u_i is the cell-specific threshold derived in Sect. 3.3.1. Estimation is carried out via the *extRemes* library in *R* (Gilleland and Katz 2016).

3.3.1 Threshold selection

The selection of an appropriate threshold above which an observation is considered extreme is a classical case of the bias-variance trade-off. Too low a threshold violates the underlying asymptotic basis and leads to bias, while too high a threshold discharges valid observations resulting in an unnecessarily high variance. A plethora of competing threshold selection techniques exist (Scarrott and MacDonald 2012). The traditional procedure is graphical via mean residual life plot (Davison and Smith 1990, MRL) which is subjective and becomes quickly infeasible for a large number of time series. An alternative by Northrop et al. (2017) proposes the use of Bayesian cross-validation, comparing thresholds based on their predictive ability at extreme levels. This method scales well while directly addressing the desired property for a threshold—if the threshold is too low, threshold excesses will not follow a GPD and predictions will be off. For this study, the size of the posterior sample simulated at each threshold is set to be 50'000 and 100 different thresholds are considered for the estimation of the quality of predictive inference. The training thresholds correspond to the 0.95–0.9995 quantiles at each GPM cell, in increments of 0.0005.

3.3.2 Dependence

Rainfall tends to occur in temporal clusters, violating the independence assumption necessary for extreme value modelling. To overcome the issue of temporal dependence, the

common method of declustering is implemented (Demirdjian et al. 2018; Gilleland and Katz 2006). The time series are declustered cell-wise such that the resulting series are near-independent if the observations are sufficiently distant in time. Such a series will have a dependence structure with no effect on the limit laws for extremes. This "runs" declustering algorithm requires first some threshold u where the values below are not considered extreme (Coles et al. 2001). Second, it starts a cluster at every first entry v with $v > u$ which runs until r consecutive observations are below u. Third, only the cluster maxima are retained and all other observations are rendered to zero. The same declustering scheme as in Demirdjian et al. (2018) is adopted, with a threshold equal to the 99-th percentile and $r = 5$.

3.3.3 Non-stationarity

The Pickands-Balkema-de Haan theorem requires the extreme values to be i.i.d. random variables which implies stationarity. Rainfall observations constitute by their very nature a non-stationary process. The PPP representation enables one to incorporate non-stationarity in the GPD parameters. In this regard, a first-order sinusoidal-function of the day of the year in the location μ and scale parameters σ is allowed, analogous to Demirdjian et al. (2018).[11] Additionally, a binary variable $STORM_{c,t}$ for cell c at time t is included to allow for a different distribution of rainfall observations that are within the spatial extent of a TC:

$$\mu_c(t) = \mu_{0,c} + \mu_{1,c} STORM_{c,t} + \mu_{2,c}\left[\sin\left(\frac{2\pi t}{365.25}\right)\right] + \mu_{3,c}\left[\cos\left(\frac{2\pi t}{365.25}\right)\right] \quad (10)$$

$$\log\left[\sigma_c(t)\right] = \sigma_{0,c} + \sigma_{1,c} STORM_{c,t} + \sigma_{2,c}\left[\sin\left(\frac{2\pi t}{365.25}\right)\right] + \sigma_{3,c}\left[\cos\left(\frac{2\pi t}{365.25}\right)\right]. \quad (11)$$

Note that, for calculating return levels of a non-stationary EV model, one has to assume values for the non-stationary parameters. Here, this is done by fixing the day of the year t and storm dummy $STORM_{c,t}$. The day of the year t is assumed to be $t = 0$ and to not influence multi-year return levels. Jamaica is on average for around 3% of the year within the outermost closed isobar of a TC. Thus, we assume that the frequency of TCs stays the same and set the storm dummy $STORM_{c,t}$ parameter equal to the sample probability $\Pr[STORM_c = 1] \approx 0.03$ for the calculation of the return levels.

3.4 Monetary return levels

The estimated return levels can be used in the damage function to obtain the n year extreme rainfall return level in monetary terms. Location of economic endowment plays also a role in the monetary risk. Average nightlight activity $W_{c,i}$ serves as weight for economic endowment, analogously to Eq. 3, where it was employed to obtain rainfall by parish per storm.[12] Projected parish i damage for a return period of r is then given by

[11] We refrain from modelling non-stationarity in the shape parameter, as it is customary in the literature.

[12] $W_{c,i}$ here is the average nightlight activity for the period 2001–2013 as opposed to the storm specific nightlight activity $W_{c,s,i}$ in Eq. 2. Specifically, $W_{c,i}$ is calculated as $W_{c,i} = \frac{\sum_{j \in c \| j \in i} w_j}{\sum_{j \in i} w_j}$, $W_{c,i} \in (0, 1)$ with $w_j = \frac{1}{|T|}\sum_{t \in T} w_{j,t}$ being the average nightlight activity in nightlight-cell j.

$$PDAMAGES_{i,r} = \beta \times \sum_{c \in i} (RAIN_{c,r} \times W_{c,i}), \tag{12}$$

where $RAIN_{c,r}$ is the estimated rainfall return level in cell c and β is the coefficient of rainfall from the damage function estimation. $PDAMAGES_{i,r}$ is the projected extreme rainfall damage during TCs in parish i that is expected to occur every r years. These parish level estimates can then be aggregated to the country level and compared to Jamaica's GDP.

4 Results

4.1 Damage function

Table 3 shows the mean damages, rainfall and wind speed per storm across parishes, whereas Appendix A.1 shows the damages by storm and parish. Hurricane Dean 2007 is associated with the strongest winds, while storm Nicole 2010 brought the heaviest rainfall to Jamaica. These two storms were also the most damaging of the five storms. Figure 1 displays the co-occurrence of rainfall, wind speed, nightlight activity and damages of Hurricane Sandy. Both rainfall and wind are the strongest in the north-east. Heaviest rainfall has been observed slightly more inland compared to wind speed, which peaked at the coast. While there is a strong relationship between the two, it is evident that these are two distinct physical phenomena with distinct spatial distribution. The map depicting nightlights clearly outlines the capital city of Kingston as the largest convolution of nightlights. A comparison with the map of damages suggests that parishes which undergo severe economic damages are also those with more nightlight activity, high winds and much rainfall.

4.1.1 Regression results

Estimates of the regression specified in Sect. 3.2.4 are displayed in Table 4. Baseline regression (1) (given by Eq. 6) shows max. wind speed to be a significant predictor of parish level damages while both maximum and total rainfall are insignificant. Since the latter two are highly collinear,[13] we consider them separately by estimating Eq. 6 without either $MRAIN_{i,s}$ or $SRAIN_{i,s}$ in columns (2) and (3), respectively. Accordingly, total rainfall during a storm is an imprecise predictor of damages. Maximum rainfall in regression (3), in contrast, is a statistically significant (10%-level) determinant of damages. Switching from parish fixed effects, which reduce the degrees of freedom considerably, to alternatively including parish population as in Eq. 7 for regression (4) yields virtually the same result. Furthermore, results do not change significantly in regression (5), based on the same Eq. 7 but without outliers as defined by Cook's Distance. The R^2 and adjusted R^2 are higher in models (1)–(3) compared to (4) and (5).[14] Since there are twelve parish indicators compared to one variable for population, the R^2 is expected to fall. The adjusted R^2 takes this

[13] The linear correlation coefficient is 0.9 and Spearman's rank correlation is 0.89. Note that, the other variables are near independent. Pearson's correlation coefficient is − 0.07 between max. wind speed and max. rainfall, 0.05 between max. wind speed and population and 0.11 between max. rainfall and population. Thus, we do not expect to have issues with collinearity besides the one already mentioned.

[14] The R^2 is the proportion of variation in the dependent variable that is explained by the independent variables. The adjusted R^2 further takes into account the reduction in degrees of freedom.

change in degrees of freedom into account—one would thus expect that the adjusted R^2 in (4) and (5) should not be lower than in (1)–(3). This is not the case. Likely, the parish indicators contain more information than just the population number and thus a model that contains these indicators will have a higher R^2. From a model selection perspective, the Bayesian Information Criterion (BIC) favours model (4) and (5).[15]

4.2 Extreme value modelling

4.2.1 Threshold and parameter estimates

The average threshold chosen by the Bayesian cross-validation is 3.24 mm/h. However, the selected thresholds are spatially heterogeneous as depicted in Fig. 2. This highlights the extent to which meteorological conditions vary across the island. Two examples of the model fitting are given in Fig. 3. Panel (a) shows the diagnostic plot for the cell that covers the capital city of Kingston close to the Blue Mountains, while panel (b) shows the diagnostic plot for the cell with the lowest 40 year return level (which is a candidate for potential threshold-misspecification). The plots show estimated measures of predictive performance, normalized to sum to 1, against training threshold. In panel (a), the highest threshold weight and thus the selected threshold is at 0.56 mm/h, while panel (b) peaks at 0.49 mm/h.[16] We see that both plots give most mass of threshold weight to values in the range of $0.5 - 3$ mm/h. As such, the specific choice of threshold appears not to have a large impact on the results as long as the threshold is within a certain range.

Parameter estimates from the extreme value GPD models are shown as boxplots in Fig. 4. The estimated GPD's are shifted to the right (large μ), smoothly decreasing ($\sigma \gg 0$), are not degenerate[17] and have a mean ($\xi \leq 1$). Estimates of the non-stationary parameters can be found in Appendix A.3.

4.2.2 Return levels

Return levels are summarized in the maps in Fig. 5. The spatial pattern over different return periods stays the same with an increase in the average level as we extrapolate to less frequent events. The highest return levels can be found in the north-eastern parish of Portland, around the city of Port Antonio.

We use the coefficient of 0.22 from the fourth column damage function regression in Table 4 as the damage function parameter to calculate predicted monetary damages in Fig. 6. These can be summed up to the country level: projected damages are for 5, 10, 20 and 40 year return periods 138.3 Mio. USD (0.9% of Jamaica's 2019 GDP), 183.1 Mio. USD (1.1%), 238.0 Mio. USD (1.5%) and 306.5 Mio. USD (1.9%), respectively.

[15] Note that, a smaller BIC means a smaller information loss relative to the true (data generating) model. Thus, one typically selects the model with smallest BIC.

[16] The x-axis is scaled on the quantiles, thus the relative distance between the two plots is hard to compare.

[17] If $\xi \ll 0$, then the GPD's support is $0 \leq x \leq -1/\xi$ and is, in the case of extreme rainfall, degenerate.

Table 3 Mean Parish Statistics per Storm

Unit	Damage Mio. USD	Max. rain (mm/h)	Total rain (mm)	Max. wind (km/h)
Michelle 2001	5.17	7.75	23.32	61.96
Dean 2007	31.99	18.33	48.45	195.19
Gustav 2008	19.50	13.99	62.26	72.14
Nicole 2010	21.87	40.49	112.91	18.25
Sandy 2012	10.83	22.96	85.82	83.33

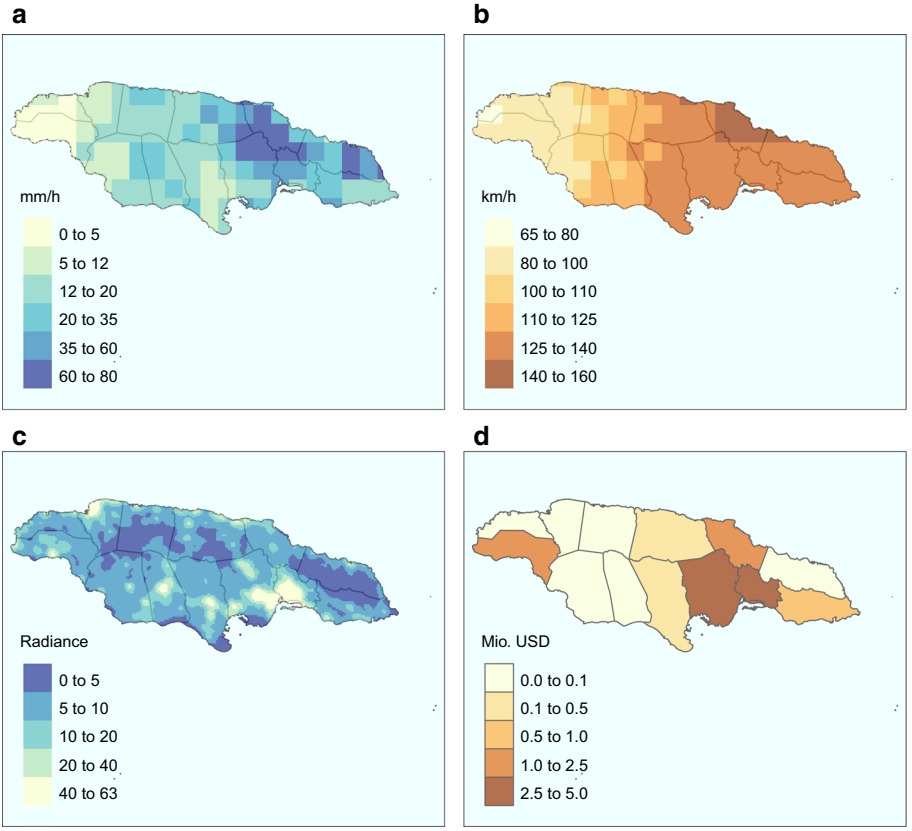

Fig. 1 Cell-wise maximum hourly rainfall (**a**) and maximum wind speed (**b**) during Hurricane Sandy 2012, average monthly nightlight intensity 2000–2013 normalized to 0–63 (**c**) and parish level damages of Hurricane Sandy 2012 (**d**)

5 Discussion

This paper makes three contributions. It adds to the recent literature that acknowledges the importance of rainfall in a TC damage function, especially with regard to climate change interactions. Employing the recent, high-resolution GPM rainfall data for an extreme value analysis in Jamaica identify the spatial distribution of extreme rainfall. Lastly, we propose

Table 4 Regression Results

	Dependent Variable: Damages in Mio. USD				
	(1)	(2)	(3)	(4)	(5)
$MRAIN_{i,s}$	0.13 (0.48)		0.24* (0.15)	0.22* (0.12)	0.23** (0.12)
$SRAIN_{i,s}$	0.05 (0.20)	0.09 (0.07)			
$MWIND^3_{i,s}/10^3$	0.01*** (0.00)	0.01*** (0.00)	0.01*** (0.00)	0.01*** (0.00)	0.01*** (0.00)
POP_i				0.03*** (0.01)	0.03*** (0.01)
$PARISH_i$	Y	Y	Y		
OUTLIER					Y
Constant	9.15 (6.87)	8.54 (5.90)	10.03 (6.82)	1.32 (3.95)	1.45 (3.97)
Observations	65	65	65	65	63
R^2	0.57	0.57	0.57	0.39	0.41
Adjusted R^2	0.45	0.45	0.45	0.36	0.37
BIC	567	562	562	538	522

*$p < 0.1$; **$p < 0.05$; ***$p < 0.01$

Standard errors in parentheses clustered by storm

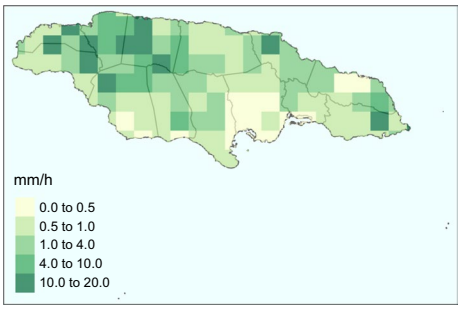

Fig. 2 Map of the selected thresholds by Bayesian cross-validation detailed in Sect. 3.3.1 by rainfall cell

a simple approach to combine the damage function with return levels and transform them into monetary risk.

The estimated linear coefficient suggests that if maximum rainfall during a TC increases by 1 mm/h in a parish, the inflicted damage increases by 0.22 Mio. USD. Depending on the TC, this can constitute a sizeable part of damages. On average for these five storms, ex post projected max. rainfall damages are 25.5% of total damages.[18] However, there can be considerable differences, depending also on the wind exposure during the storm: the average contribution of max. wind speed is 34%, while residual damages are 40.5%.[19] For example, during tropical storm Nicole in 2010, the average parish max. rainfall was 40.5 mm/h, which translates into 8.9 Mio. USD, while average parish damages were 21.9 Mio. USD. In contrast, when Hurricane Dean brought strong winds over the island of Jamaica

[18] That is calculated as the fraction of projected damages against total reported damages.

[19] Damages not explained in the model come from factors such as storm surge and residual variation in the data.

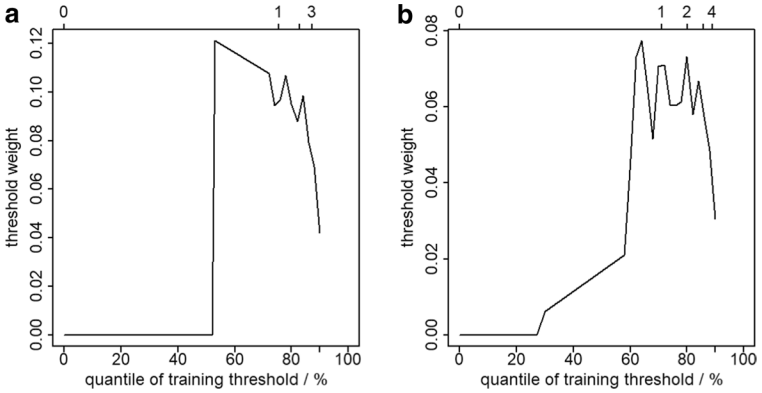

Fig. 3 Example diagnostic plots of estimated measures of predictive performance. **a** shows the threshold selection for the cell centred at (18.05, −76.75) which is a cell that covers the capital of Kingston where it is close to the Blue Mountains. **b** shows the threshold selection for the cell centred at (17.95, −77.25) which exhibits the lowest 40 year return level. Quantiles of training threshold relate to the subset of nonzero entries in order to provide interpretable information. For details about the procedure to produce the plots, see Eqs. (7) and (14) in Northrop et al. (2017)

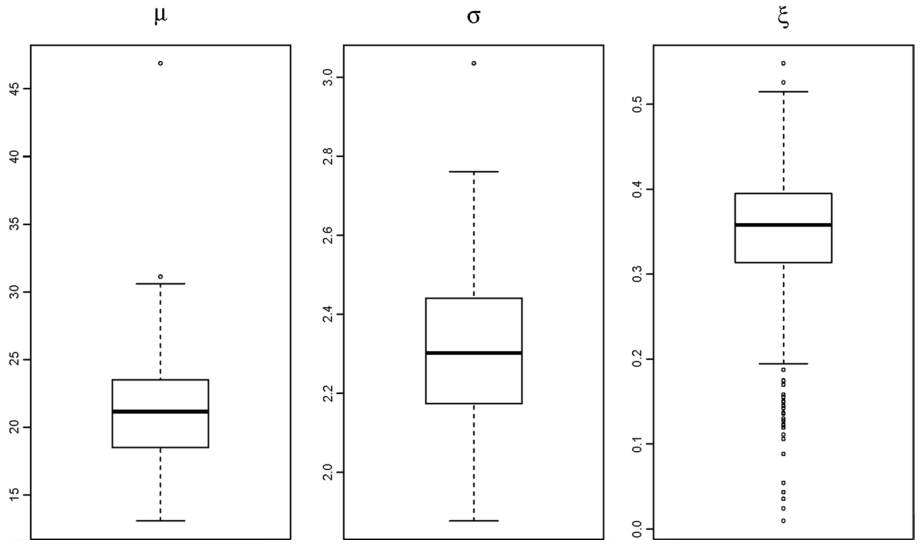

Fig. 4 Boxplot of the location μ, scale σ and ξ parameter under the non-stationarity assumption as discussed in Sect. 3.3.3

in 2007, the average parish max. rainfall was only 18.3 mm/h resulting 4 Mio. USD damages (compared to the average 32 Mio. USD per parish), while 67% (21.4 Mio. USD) can be attributed to max. wind speed. This supports the view expressed in Eberenz et al. (2021) that wind-only damage functions fail to predict the destruction of rainfall heavy TCs. When comparing the observed events to the risk estimates, the extreme value analysis suggests that a rainfall heavy event like Nicole in 2010 has a lower return period than 10 years. If

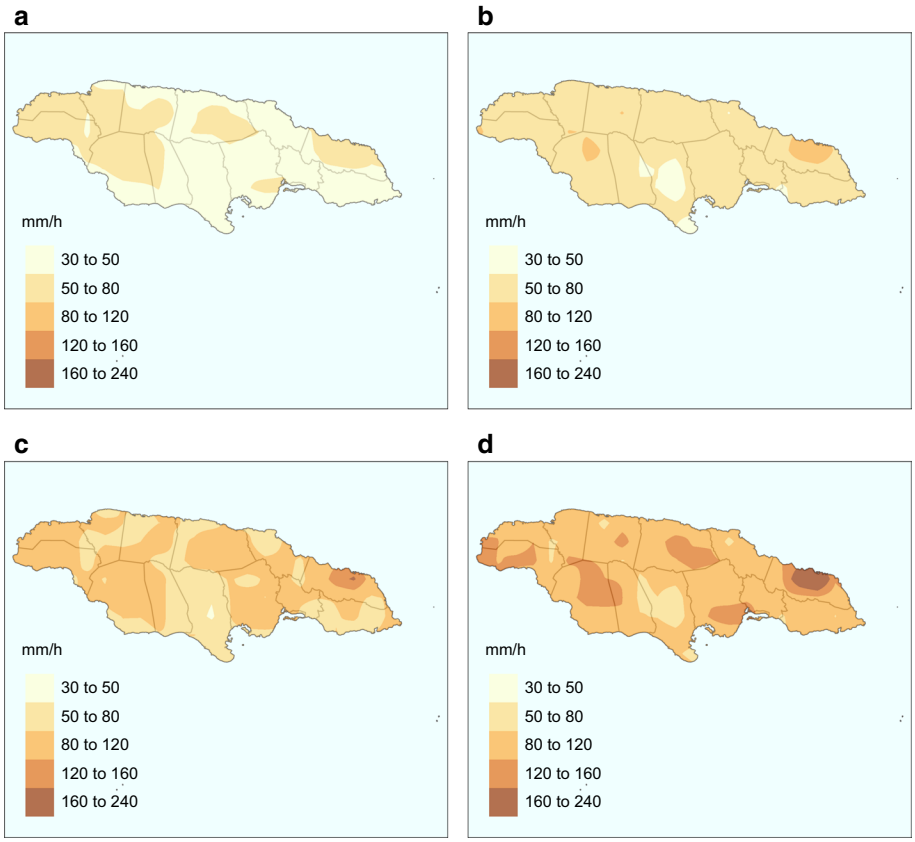

Fig. 5 Maps depicting 5 (**a**), 10 (**b**), 20 (**c**) and 40 year return levels. The contour-type maps are drawn by disaggregating every cell into 64 sub-cells which are then bilinearly interpolated

extrapolated to less frequent events with a 20 or 40 year return period, the potential damages due to rainfall quickly dwarf those observed in any of the storms are examined.

It is insightful to compare the return level estimates to those found in the literature. Demirdjian et al. (2018), who employ a PPP approach on a global scale with the TRMM data, estimate 25 year return levels in the range of 150–180 mm/h for southern Florida.[20] Burgess et al. (2015) use long rainfall time series of two airports in Jamaica and estimate the 30 min. 25 year return level to be 110 and 128 mm/h, respectively. In comparison, if we consider the location of these two airports (Montego Bay and Kingston), the 20 year return level estimated in this analysis is around 80 to 90 mm/h for both.[21] Unsurprisingly, we find that the area north of the Blue Mountains is most susceptible to extreme rainfall during a TC. This is likely because TCs often first make landfall in the north-east of Jamaica. Orographic lift of the Blue Mountains in the north-eastern parishes increases the prevalence of heavy rainfall in that area further (Laing 2004).

[20] Note that, the TRMM data is 3-hourly compared to the half-hourly GPM.

[21] The cities are in more than one grid cell.

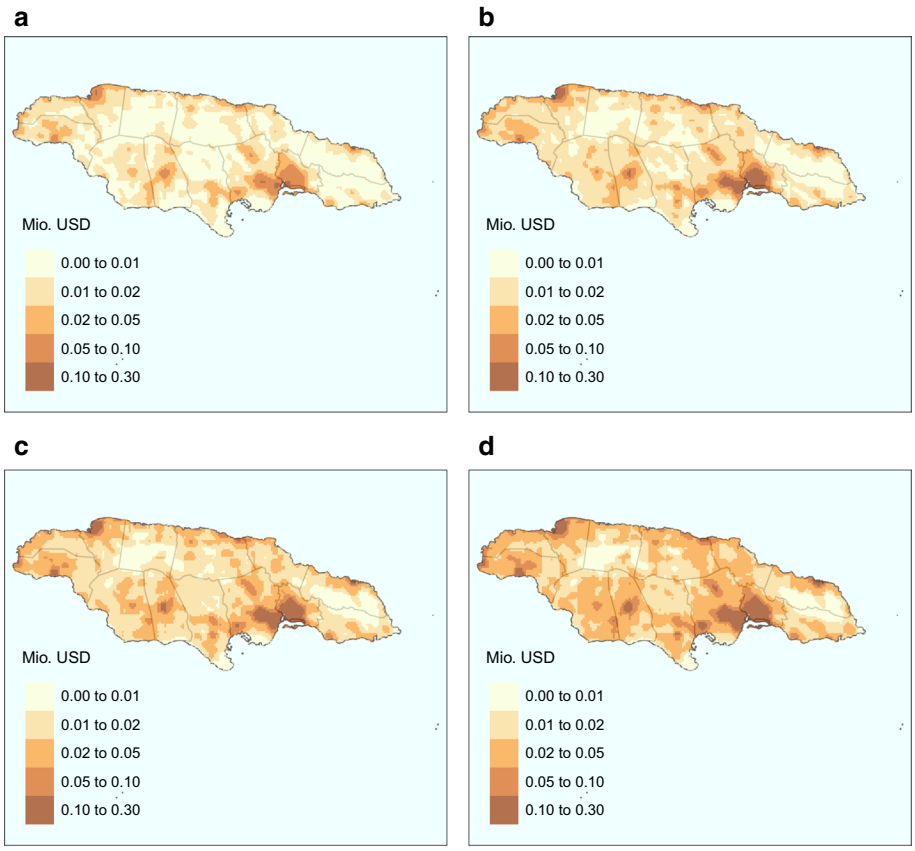

Fig. 6 Maps depicting 5 (**a**), 10 (**b**), 20 (**c**) and 40 year projected damages calculated as shown in Eq. 12

Our risk estimates could arguably be useful for policy. More precisely, from a damage mitigation perspective, modelling the spatial distribution of risk is necessary for the planning and execution of ex-ante mitigation interventions (Holcombe and Anderson 2010; Anderson et al. 2011). For example, we find that the north-eastern parish of Portland is most susceptible to extreme rainfall and should therefore be a priority area for preventive measures such as proper surface water management to decrease landslide risk. Nevertheless, while our damage estimates serve to give an indication of the loss of assets from extreme precipitation during a TC, one should note that they only constitute part of the economic impact. More specifically, the direct damages are likely to result also in indirect damages through disruption of economic activity (Hallegatte and Przyluski 2010). Strobl (2012) for example estimates the macroeconomic reduction in output for the average hurricane strike in the Central American and Caribbean region to be at least 0.83 percentage points, although this estimate was solely based on damages due to wind exposure. The estimates here suggest that projected direct damages for a 5 and 40 year return period event are in value 0.9% and 1.9% of Jamaica's GDP. However, these figures cannot a priori tell us how the damages will translate into changes in aggregate output as this will depend on the indirect consequences, disaster relief and whether the damaged assets are replaced, among others. For instance, Lenzen et al. (2019) show that TC Debby 2017 caused significant

disruption through the supply chain to regions and industries in Australia that were not themselves hit by the storm. These spillover effects could be an avenue for future research.

There are a number of weaknesses inherent in our methodological approach that future research could address. Firstly, the magnitude of the projected damages crucially depends on the damage function estimate for extreme rainfall. While the coefficient of interest in Table 4 does not change statistically significant across specifications (3)–(5),[22] there are still a number of caveats to be made in this approach. First, both the dependent variable (reported damages) and the independent variables are subject to measurement error.[23] Measurement error in the dependent variable is less problematic (if it is not systematic) since it "only" increases the unexplainable part of the regression and will simply result in less precise estimates. Measurement error in the extreme rainfall, our independent variable of interest, is more of a concern since a sufficient amount of such will induce attenuation bias of the estimates towards zero (Frost and Thompson 2000). A second caveat is the focus on statistical modelling and the omission of a hydrological perspective. Extreme rainfall during TCs is itself not a hazard but the cause for hazards such as floods and landslides (Yumul et al. 2012; Nolasco-Javier et al. 2015; Nolasco-Javier and Kumar 2018). Hydrological models would be able to decipher this relationship more precisely. The challenge of employing a hydrological model instead of a statistical approach is, however, in terms of feasibility and generalizability. Complete multi-hazard large-scale hydrological models are still an active research area (Lung et al. 2013; Koks et al. 2019). With the additional complexity of a model that makes use of the extent of river catchments, local soil type and hill slopes, any result from the analysis could only be in terms of these specific conditions. The precision gained by a realistic model is thus paid with a narrower transferability of the results. The last restriction concerns the valuation of non-monetary damages. More specifically, the monetary damages figures used here do not account for other non-monetized impacts like the erosion and deterioration of soil which can be linked to extreme rainfall events (Rawlins et al. 1998), as well as psychological and mental health impacts to the exposed population (Lindell and Prater 2003; Bourque et al. 2006).

6 Conclusion

While the overall effect of climate change on the frequency and severity of TCs is a matter of debate and may be ocean basin specific, there is a general consensus that rainfall heavy TCs will likely become more common with global warming (Grossmann and Morgan 2011; Walsh et al. 2016; Knutson et al. 2019). In considering what greater precipitation in future TCs will mean in terms of economic impact, much of the current literature has focused on estimating the impact in terms of wind-induced damages. Even if one assumes that wind is a sufficient proxy for TC damages, a wind-only damage function likely underestimates future damage in climate change scenarios. The analysis presented in this case study of Jamaica shows that extreme rainfall during TCs is also potentially an important driver. Depending on the specification, a conservative estimate suggests that rainfall during a TC causes direct damage of 1.5% of GDP for a 20 year event. Thus, failing to take

[22] A Wald-test of the preferred model (4)'s coefficient (0.22) against the coefficient from model (3) cannot reject their equality at any conventional level (p value = 0.82).

[23] Damages are constructed and interpolated from incomplete reports, as discussed in Sect. 2.2. Wind and rainfall observations are constructed from a parametric model or remote sensing information, and both are aggregated to a larger spatial scale. All these steps in the data construction are sources of measurement error.

account of extreme precipitation in risk assessments may not only underestimate future damage but substantially bias current risk assessment.

Appendix

Panel summary statistics

See Tables 5, 6, 7, 8, 9.

Table 5 Hurricane Michelle storm statistics

Unit	Damage (Mio. USD)	Max. Rain (mm/h)	Total Rain (mm)	Max. Wind (km/h)	Population (1'000)
Clarendon	2.38	3.39	9.49	61.02	245.10
Hanover	1.51	4.98	17.93	69.56	69.53
Manchester	1.36	3.47	10.73	61.59	189.80
Portland	9.41	26.24	70.16	52.10	81.74
St. Andrew & Kingston	20.49	7.90	22.79	58.99	662.43
St. Ann	3.20	8.82	26.04	63.35	172.36
St. Catherine	3.91	3.39	8.95	59.95	516.22
St. Elizabeth	4.86	5.38	13.95	64.62	150.21
St. James	2.48	2.80	12.55	68.24	93.90
St. Mary	11.79	17.06	51.19	60.61	113.61
St. Thomas	2.47	6.85	27.72	50.05	93.90
Trelawny	1.62	5.28	14.56	66.79	75.16
Westmoreland	1.77	5.24	17.14	68.67	144.10

Table 6 Hurricane Dean storm statistics

Unit	Damage Mio. USD	Max. Rain (mm/h)	Total Rain (mm)	Max. Wind (km/h)	Population (1'000)
Clarendon	63.31	20.65	63.11	212.31	245.10
Hanover	10.61	12.15	37.07	184.64	69.53
Manchester	59.98	22.29	64.19	213.99	189.80
Portland	6.69	18.88	46.15	173.90	81.74
St. Andrew & Kingston	49.05	18.45	52.94	196.53	662.43
St. Ann	18.91	16.24	43.06	187.85	172.36
St. Catherine	33.34	20.93	58.62	200.10	516.22
St. Elizabeth	36.22	12.16	35.64	218.23	150.21
St. James	18.89	10.84	29.67	196.60	93.90
St. Mary	22.87	21.94	47.19	179.63	113.61
St. Thomas	51.80	26.71	59.31	184.71	93.90
Trelawny	13.05	20.49	49.72	192.85	75.16
Westmoreland	31.19	16.61	43.22	196.08	144.10

Table 7 Storm Gustav storm statistics

Unit	Damage Mio. USD	Max. Rain (mm/h)	Total Rain (mm)	Max. Wind (km/h)	Population (1'000)
Clarendon	19.22	13.16	66.25	71.24	245.10
Hanover	6.43	9.13	50.90	71.23	69.53
Manchester	3.43	11.88	57.70	74.06	189.80
Portland	3.55	24.13	79.69	71.88	81.74
St. Andrew & Kingston	57.04	13.67	80.60	70.99	662.43
St. Ann	2.41	14.32	58.53	71.10	172.36
St. Catherine	34.39	17.18	67.66	71.08	516.22
St. Elizabeth	5.06	7.29	45.06	75.84	150.21
St. James	8.39	9.56	41.65	72.37	93.90
St. Mary	47.06	14.33	88.08	71.63	113.61
St. Thomas	24.80	31.49	82.28	70.88	93.90
Trelawny	1.66	7.88	45.39	74.45	75.16
Westmoreland	40.07	7.77	45.54	71.05	144.10

Table 8 Storm Nicole storm statistics

Unit	Damage Mio. USD	Max. Rain (mm/h)	Total Rain (mm)	Max. Wind (km/h)	Population (1'000)
Clarendon	23.60	44.62	120.05	18.71	245.10
Hanover	9.03	22.11	82.52	21.26	69.53
Manchester	14.39	33.98	110.84	19.11	189.80
Portland	35.85	23.24	71.27	13.16	81.74
St. Andrew & Kingston	38.91	48.35	100.30	17.24	662.43
St. Ann	16.41	51.84	117.43	18.97	172.36
St. Catherine	24.57	56.75	123.19	17.83	516.22
St. Elizabeth	28.48	51.61	156.35	19.60	150.21
St. James	16.48	34.86	120.90	20.17	93.90
St. Mary	26.81	24.06	64.41	18.71	113.61
St. Thomas	16.27	21.86	72.53	11.30	93.90
Trelawny	8.21	77.84	197.15	20.15	75.16
Westmoreland	25.33	35.25	130.96	21.08	144.10

Wind field model

In terms of implementing Eq. (1), one should note that the maximum sustained wind velocity anywhere in the storm $V_{m,s,t}$ is given by the storm track data, the forward velocity of the storm $V_{h,s,t}$ can be directly calculated by following the storm's movements between successive locations along its track, and the radial distance $R_{c,s,t}$ and the clockwise angle $T_{c,s,t}$ are calculated relative to the point of interest c. All other parameters

Table 9 Hurricane Sandy storm statistics

Unit	Damage Mio. USD	Max. Rain (mm/h)	Total Rain (mm)	Max. Wind (km/h)	Population (1'000)
Clarendon	3.25	12.95	85.69	87.72	245.10
Hanover	0.57	4.50	12.23	63.74	69.53
Manchester	0.68	18.21	96.09	78.98	189.80
Portland	0.20	52.07	169.02	96.25	81.74
St. Andrew & Kingston	10.74	38.78	133.27	95.92	662.43
St. Ann	4.47	30.89	102.31	90.88	172.36
St. Catherine	26.85	27.99	107.04	92.45	516.22
St. Elizabeth	0.23	13.51	59.39	72.04	150.21
St. James	1.82	8.38	26.90	71.28	93.90
St. Mary	30.84	51.34	130.15	101.62	113.61
St. Thomas	26.85	17.54	120.78	93.75	93.90
Trelawny	1.41	17.21	59.93	75.13	75.16
Westmoreland	32.90	5.06	12.92	63.57	144.10

have to be estimated or values assumed. For instance, we have no information on the gust wind factor G, but a number of studies (see, e.g. Paulsen and Schroeder 2005) have measured G to be around 1.5, and we also use this value. For S, we follow Boose et al. (2004) and assume it to be 1. While we also do not know the surface friction to directly determine D, Vickery et al. (2009) note that in open water, the reduction factor is about 0.7 and reduces by 14% on the coast and 28% further 50 km inland. We thus adopt a reduction factor that decreases linearly within this range as we consider points c further inland from the coast. Finally, to determine the shape of the wind profile curve B, we employ the approximation method of Holland (1980) where B is assumed to be in the range of 1.5–2.5 and negatively correlated with central pressure. We use the parametric model estimated by Xiao et al. (2009) to estimate the radius of maximum winds $R_{m,s,t}$.

PPP parameter estimates

Figures 7 and 8.

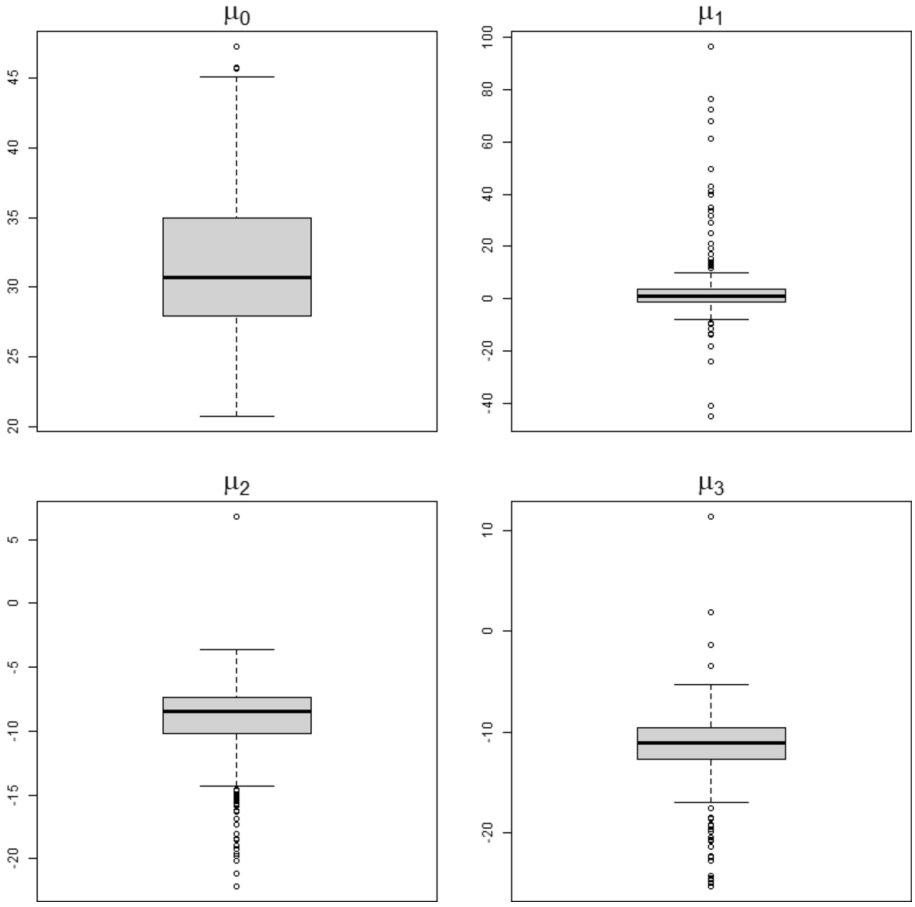

Fig. 7 Boxplot of the location parameters as outlined in Eqs. 10 and 11

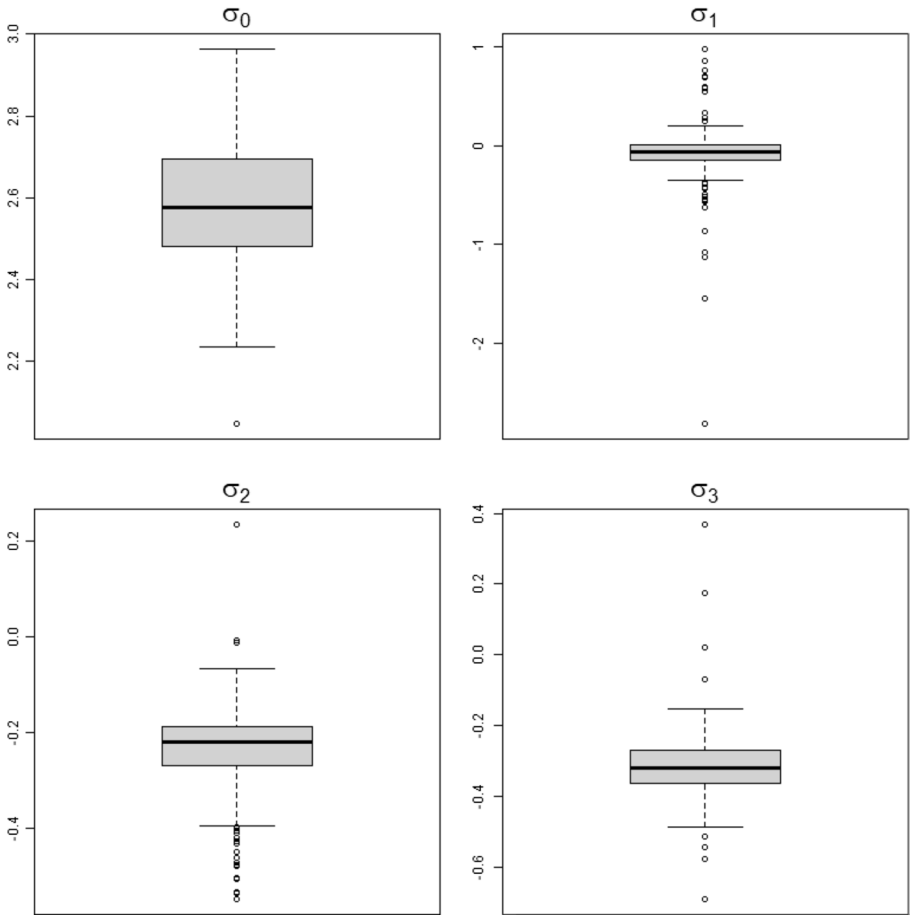

Fig. 8 Boxplot of the scale parameters as outlined in Eqs. 10 and 11

Acknowledgements Our thank goes to participants of the Brown Bag Seminar of the Department of Economics at University of Bern for valuable comments and attendees of the "Natural Disasters and Climate Change" panel at the 25th Annual Conference of the European Association of Environmental and Resource Economists for discussion and inputs. Special thanks goes to Jeanne Tschopp for her input at an early stage of the manuscript that helped mature the work.

Funding information Open Access funding provided by Universität Bern. No funding was received for conducting this study.

Data availability The primary data used or analysed in this study are freely available at the indicated source. Data that result through the application of the methodology in this work are available from the corresponding author on reasonable request.

Declarations

Conflict of interest The authors declare that they have no conflict of interest.

Code availability (software application or custom code) The majority of the analysis was conducted in *R*, a free software environment for statistical computing and graphics. The extreme value modelling relies heavily

on the free *R* library *extRemes*. Data from remote sensing sources have been prepared in version 1.9 of the free Climate Data Operators (CDO) program by the Max-Planck-Institute on Linux. On reasonable request, *R* scripts that were used to perform the analysis can be obtained from the corresponding author.

References

Anderson MG, Holcombe E, Blake JR, Ghesquire F, Holm-Nielsen N, Fisseha T (2011) Reducing landslide risk in communities: Evidence from the eastern caribbean. Appl Geogr 31(2):590–599

Bakkensen LA, Park DSR, Sarkar RSR (2018) Climate costs of tropical cyclone losses also depend on rain. Environ Res Lett 13(7):074034

Baradaranshoraka M, Pinelli JP, Gurley K, Peng X, Zhao M (2017) Hurricane wind versus storm surge damage in the context of a risk prediction model. J Struct Eng 143(9):04017103

Beguería S, Angulo-Martínez M, Vicente-Serrano SM, López-Moreno JI, El-Kenawy A (2011) Assessing trends in extreme precipitation events intensity and magnitude using non-stationary peaks-over-threshold analysis: a case study in northeast spain from 1930 to 2006. Int J Climatol 31(14):2102–2114

Bertinelli L, Strobl E (2013) Quantifying the local economic growth impact of hurricane strikes: an analysis from outer space for the Caribbean. J Appl Meteorol Climatol 52(8):1688–1697

Boose E, Serrano M, Foster D (2004) Landscape and regional impacts of hurricanes in Puerto Rico. Ecol Monogr 74:335–352

Bourque LB, Siegel JM, Kano M, Wood MM (2006) Weathering the storm: The impact of hurricanes on physical and mental health. Annals Am Acad Polit Soc Sci 604(1):129–151

Bradshaw S (2003) Handbook for estimating the socio-economic and environmental effects of disasters. ECLAC & International Bank for Reconstruction & Development

Burgess CP, Taylor MA, Stephenson T, Mandal A (2015) Frequency analysis, infilling and trends for extreme precipitation for Jamaica (1895–2100). J Hydrol: Reg Stud 3:424–443

Carby B (2018) Integrating disaster risk reduction in national development planning: experience and challenges of jamaica. Environ Hazards 17(3):219–233

Chen SS, Knaff JA, Marks FD Jr (2006) Effects of vertical wind shear and storm motion on tropical cyclone rainfall asymmetries deduced from trmm. Mon Weather Rev 134(11):3190–3208

Chen X, Nordhaus WD (2011) Using luminosity data as a proxy for economic statistics. Proc Natl Acad Sci 108(21):8589–8594

Coles S, Bawa J, Trenner L, Dorazio P (2001) An introduction to statistical modeling of extreme values, vol 208. Springer, Berlin

Collischonn B, Collischonn W, Tucci CEM (2008) Daily hydrological modeling in the amazon basin using trmm rainfall estimates. J Hydrol 360(1–4):207–216

Conceição P (2019) Human Development Report 2019: Beyond Income, Beyond Averages, Beyond Today: Inequalities in Human Development in the 21st Century. United Nations Development Programme

Cook RD (1977) Detection of influential observation in linear regression. Technometrics 19(1):15–18, http://www.jstor.org/stable/1268249

Czajkowski J, Simmons K, Sutter D (2011) An analysis of coastal and inland fatalities in landfalling us Hurricanes. Nat Hazards 59(3):1513–1531

Davison AC, Smith RL (1990) Models for exceedances over high thresholds. J Royal Stat Soc: Ser B (Methodol) 52(3):393–425

Demirdjian L, Zhou Y, Huffman GJ (2018) Statistical modeling of extreme precipitation with trmm data. J Appl Meteorol Climatol 57(1):15–30

Demuth J, DeMaria M, Knaff J (2006) Improvement of advanced microwave sounding unit tropical cyclone intensity and size estimation algorithms. J Appl Meteorol

Do TQ, van de Lindt JW, Cox DT (2020) Hurricane surge-wave building fragility methodology for use in damage, loss, and resilience analysis. J Struct Eng 146(1):04019177
Dou J, Yunus AP, Xu Y, Zhu Z, Chen CW, Sahana M, Khosravi K, Yang Y, Pham BT (2019) Torrential rainfall-triggered shallow landslide characteristics and susceptibility assessment using ensemble data-driven models in the dongjiang reservoir watershed, china. Nat Haz 97(2):579–609
Eberenz S, Lüthi S, Bresch DN (2021) Regional tropical cyclone impact functions for globally consistent risk assessments. Nat Haz Earth Syst Sci 21(1):393–415
Elliott RJ, Strobl E, Sun P (2015) The local impact of typhoons on economic activity in China: A view from outer space. J Urban Econ 88:50–66
Emanuel K (2005) Increasing destructiveness of tropical cyclones over the past 30 years. Nat 436(7051):686
Emanuel KA (2013) Downscaling cmip5 climate models shows increased tropical cyclone activity over the 21st century. Proc Natl Acad Sci 110(30):12219–12224
Frost C, Thompson SG (2000) Correcting for regression dilution bias: comparison of methods for a single predictor variable. J Royal Stat Soc: Ser A (Stat Soc) 163(2):173–189
Furrer EM, Katz RW (2008) Improving the simulation of extreme precipitation events by stochastic weather generators. Wat Resour Res 44(12)
Gilleland E, Katz RW (2006) Gilleland E, Katz RW (2006) Analyzing seasonal to interannual extreme weather and climate variability with the extremes toolkit. In: 18th Conference on Climate Variability and Change, 86th American Meteorological Society (AMS) Annual Meeting, Citeseer, vol 29
Gilleland E, Katz RW (2016) extRemes 2.0: An extreme value analysis package in R. J Stat Softw 72(8):1–39
Grossmann I, Morgan MG (2011) Tropical cyclones, climate change, and scientific uncertainty: what do we know, what does it mean, and what should be done? Clim Chang 108(3):543–579
Hallegatte S, Przyluski V (2010) The economics of natural disasters: concepts and methods. The World Bank, Washington
Hatzikyriakou A, Lin N (2018) Assessing the vulnerability of structures and residential communities to storm surge: An analysis of flood impact during hurricane sandy. Front Built Environ 4:4
Hence DA, Houze RA Jr (2011) Vertical structure of hurricane eyewalls as seen by the trmm precipitation radar. J Atmos Sci 68(8):1637–1652
Hendricks EA, Peng MS, Fu B, Li T (2010) Quantifying environmental control on tropical cyclone intensity change. Mon Weather Rev 138(8):3243–3271
Holcombe E, Anderson M (2010) Tackling landslide risk: Helping land use policy to reflect unplanned housing realities in the eastern caribbean. Land Use Policy 27(3):798–800
Holland G (1980) An analytic model of the wind and pressure profiles in Hurricanes. Mon Weather Rev 106:1212–1218
Hou AY, Kakar RK, Neeck S, Azarbarzin AA, Kummerow CD, Kojima M, Oki R, Nakamura K, Iguchi T (2014) The global precipitation measurement mission. Bull Am Meteorol Soc 95(5):701–722
Hu X, Liu B, Wu ZY, Gong J (2016) Analysis of dominant factors associated with hurricane damages to residential structures using the rough set theory. Nat Hazards Rev 17(3):04016005
Huffman GJ, Bolvin DT, Nelkin EJ, Wolff DB, Adler RF, Gu G, Hong Y, Bowman KP, Stocker EF (2007) The trmm multisatellite precipitation analysis (tmpa): Quasi-global, multiyear, combined-sensor precipitation estimates at fine scales. J Hydrometeorol 8(1):38–55
Huffman GJ, Bolvin DT, Braithwaite D, Hsu K, Joyce R, Xie P, Yoo SH (2015a) Nasa global precipitation measurement (gpm) integrated multi-satellite retrievals for gpm (imerg). Algorithm Theor Basis Doc, Version 4:30
Huffman GJ, Bolvin DT, Nelkin EJ et al (2019) (2015b) Integrated multi-satellite retrievals for gpm (imerg) technical documentation. NASA/GSFC Code 612(47)
Huffman GJ, Bolvin DT, Nelkin EJ, Jackson T (2020) Integrated multi-satellite retrievals for gpm (imerg). technical documentation. Tech. rep., Mesoscale Atmospheric Processes Laboratory. Science Systems and Applications Inc., NASA Goddard Space Flight Center
Jiang H, Halverson JB, Simpson J, Zipser EJ (2008) Hurricane rainfall potential derived from satellite observations aids overland rainfall prediction. J Appl Meteorol Climatol 47(4):944–959
Jiang H, Liu C, Zipser EJ (2011) A trmm-based tropical cyclone cloud and precipitation feature database. J Appl Meteorol Climatol 50(6):1255–1274
Johnston J, Montecino JA (2012) Update on the Jamaican economy. Center for Economic and Policy Research, Washington DC
Knutson T, Camargo SJ, Chan JC, Emanuel K, Ho CH, Kossin J, Mohapatra M, Satoh M, Sugi M, Walsh K (2019) Tropical cyclones and climate change assessment: Part i: Detection and attribution. Bull Am Meteorol Soc 100(10):1987–2007

Koks EE, Rozenberg J, Zorn C, Tariverdi M, Vousdoukas M, Fraser S, Hall J, Hallegatte S (2019) A global multi-hazard risk analysis of road and railway infrastructure assets. Nat Commun 10(1):1–11
Laing AG (2004) Cases of heavy precipitation and flash floods in the Caribbean during el nino winters. J Hydrometeorol 5(4):577–594
Landsea CW, Franklin JL (2013) Atlantic hurricane database uncertainty and presentation of a new database format. Mon Wearther Rev 141:3576–3592
Larsen MC, Simon A (1993) A rainfall intensity-duration threshold for landslides in a humid-tropical environment, Puerto Rico. Geografiska Annaler: Ser A, Phys Geogr 75(1–2):13–23
Lau KM, Zhou Y, Wu HT (2008) Have tropical cyclones been feeding more extreme rainfall? J Geophys Res: Atmos 113(D23)
Lenzen M, Malik A, Kenway S, Daniels P, Lam KL, Geschke A (2019) Economic damage and spillovers from a tropical cyclone. Nat Hazards Earth Syst Sci 19(1):137–151
Li XH, Zhang Q, Xu CY (2012) Suitability of the trmm satellite rainfalls in driving a distributed hydrological model for water balance computations in xinjiang catchment, poyang lake basin. J Hydrol 426:28–38
Li Y, Fang W, Duan X (2019) On the driving forces of historical changes in the fatalities of tropical cyclone disasters in China from 1951 to 2014. Nat Hazards 98(2):507–533
Lin N, Smith JA, Villarini G, Marchok TP, Baeck ML (2010) Modeling extreme rainfall, winds, and surge from Hurricane Isabel (2003). Weather Forecast 25(5):1342–1361
Lindell MK, Prater CS (2003) Assessing community impacts of natural disasters. Nat Hazards Rev 4(4):176–185
Lonfat M, Marks FD Jr, Chen SS (2004) Precipitation distribution in tropical cyclones using the tropical rainfall measuring mission (trmm) microwave imager: A global perspective. Mon Weather Rev 132(7):1645–1660
López-Marrero T, Castro-Rivera A (2019) Lets not forget about non-land-falling cyclones: tendencies and impacts in Puerto Rico. Nat Hazards 98(2):809–815
Lung T, Lavalle C, Hiederer R, Dosio A, Bouwer LM (2013) A multi-hazard regional level impact assessment for Europe combining indicators of climatic and non-climatic change. Global Environl Chang 23(2):522–536
Masoomi H, van de Lindt JW, Ameri MR, Do TQ, Webb BM (2019) Combined wind-wave-surge Hurricane-induced damage prediction for buildings. J Struct Eng 145(1):04018227
Matyas CJ, Silva JA (2013) Extreme weather and economic well-being in rural Mozambique. Nat Hazards 66(1):31–49
Miller S, Brewer T, Harris N (2009) Rainfall thresholding and susceptibility assessment of rainfall-induced landslides: application to landslide management in St. Thomas, Jamaica. Bull Eng Geol Environ 68(4):539
Murnane RJ, Elsner JB (2012) Maximum wind speeds and us hurricane losses. Geophys Res Lett 39(16)
Nkemdirim LC (1979) Spatial and seasonal distribution of rainfall and runoff in Jamaica. Geogr Rev 288–301
NOAA (2019) Noaa increases chance for above-normal hurricane season. https://www.noaa.gov/media-release/noaa-increases-chance-for-above-normal-hurricane-season
Nolasco-Javier D, Kumar L (2018) Deriving the rainfall threshold for shallow landslide early warning during tropical cyclones: a case study in Northern Philippines. Nat Hazards 90(2):921–941
Nolasco-Javier D, Kumar L, Tengonciang AMP (2015) Rapid appraisal of rainfall threshold and selected landslides in Baguio, Philippines. Nat Hazards 78(3):1587–1607
Nordhaus WD (2006) The economics of hurricanes in the United States. Tech. rep, National Bureau of Economic Research
Northrop PJ, Attalides N, Jonathan P (2017) Cross-validatory extreme value threshold selection and uncertainty with application to ocean storm severity. J Royal Stat Soc: Ser C (Appl Stat) 66(1):93–120
Park DSR, Ho CH, Nam CC, Kim HS (2015) Evidence of reduced vulnerability to tropical cyclones in the republic of Korea. Environ Res Lett 10(5):054003
Park S, van de Lindt JW, Li Y (2013) Application of the hybrid abv procedure for assessing community risk to Hurricanes spatially. Nat Hazards 68(2):981–1000
Paulsen B, Schroeder J (2005) An examination of tropical and extratropical gust factors and the associated wind speed histograms. J Appl Meteorol 44:270–280
Peduzzi P, Chatenoux B, Dao H, De Bono A, Herold C, Kossin J, Mouton F, Nordbeck O (2012) Global trends in tropical cyclone risk. Nat Clim Chang 2(4):289–294
Rappaport EN (2014) Fatalities in the united states from Atlantic tropical cyclones: New data and interpretation. Bull Am Meteorol Soc 95(3):341–346

Rawlins B, Ferguson A, Chilton P, Arthurton R, Rees J, Baldock J (1998) Review of agricultural pollution in the Caribbean with particular emphasis on small island developing states. Marine Pollut Bull 36(9):658–668
Rezapour M, Baldock TE (2014) Classification of hurricane hazards: The importance of rainfall. Weather Forecast 29(6):1319–1331
Rosenzweig BR, McPhillips L, Chang H, Cheng C, Welty C, Matsler M, Iwaniec D, Davidson CI (2018) Pluvial flood risk and opportunities for resilience. Wiley Interdiscip Rev: Water 5(6):e1302
Rözer V, Kreibich H, Schröter K, Müller M, Sairam N, Doss-Gollin J, Lall U, Merz B (2019) Probabilistic models significantly reduce uncertainty in hurricane Harvey pluvial flood loss estimates. Earth Future 7(4):384–394
Scarrott C, MacDonald A (2012) A review of extreme value threshold estimation and uncertainty quantification. REVSTAT-Stat J 10(1):33–60
Spekkers M, Kok M, Clemens F, Ten Veldhuis J (2013) A statistical analysis of insurance damage claims related to rainfall extremes. Hydrol Earth Syst Sci 17(3)
Statistical Institute of Jamaica (2011) Population usually resident in Jamaica, by parish. Population Census
Strobl E (2011) The economic growth impact of Hurricanes: evidence from US coastal counties. Rev Econ Stat 93(2):575–589
Strobl E (2012) The economic growth impact of natural disasters in developing countries: Evidence from Hurricane strikes in the central american and caribbean regions. J Dev Econ 97(1):130–141
Sugahara S, Da Rocha RP, Silveira R (2009) Non-stationary frequency analysis of extreme daily rainfall in Sao Paulo, Brazil. Int J Climatol: J Royal Meteorol Soc 29(9):1339–1349
The World Bank Group (2018) Advancing disaster risk finance in Jamaica. International Bank for Reconstruction and Development
Tramblay Y, Neppel L, Carreau J, Najib K (2013) Non-stationary frequency analysis of heavy rainfall events in southern France. Hydrol Sci J 58(2):280–294
US Bureau of Labor Statistics (2019) Consumer price index for all urban consumers: All items [cpiaucsl]
Van Oldenborgh GJ, Van Der Wiel K, Sebastian A, Singh R, Arrighi J, Otto F, Haustein K, Li S, Vecchi G, Cullen H (2017) Attribution of extreme rainfall from Hurricane Harvey, august 2017. Environ Res Lett 12(12):124009
Van Ootegem L, Verhofstadt E, Van Herck K, Creten T (2015) Multivariate pluvial flood damage models. Environ Impact Assess Rev 54:91–100
Van Ootegem L, Van Herck K, Creten T, Verhofstadt E, Foresti L, Goudenhoofdt E, Reyniers M, Delobbe L, Murla Tuyls D, Willems P (2018) Exploring the potential of multivariate depth-damage and rainfall-damage models. J Flood Risk Manag 11:S916–S929
Vickery P, Masters F, Powell M, Wadhera D (2009) Hurricane hazard modeling: The past, present, and future. J Wind Eng Ind Aerodyn 97:392–405
Villarini G, Smith JA, Baeck ML, Marchok T, Vecchi GA (2011) Characterization of rainfall distribution and flooding associated with us landfalling tropical cyclones: Analyses of hurricanes Frances, Ivan, and Jeanne (2004). J Geophys Res: Atmos: 116(D23)
Villarini G, Goska R, Smith JA, Vecchi GA (2014a) North Atlantic tropical cyclones and US flooding. Bull Am Meteorol Soc 95(9):1381–1388
Villarini G, Lavers DA, Scoccimarro E, Zhao M, Wehner MF, Vecchi GA, Knutson TR, Reed KA (2014b) Sensitivity of tropical cyclone rainfall to idealized global-scale Forcings. J Clim 27(12):4622–4641
Walsh KJ, McBride JL, Klotzbach PJ, Balachandran S, Camargo SJ, Holland G, Knutson TR, Kossin JP, Lee Tc, Sobel A, Sugi M (2016) Tropical cyclones and climate change. Wiley Interdiscip Rev: Clim Chang 7(1):65–89
(2020) Population, total - latin america & caribbean. World Bank Group https://data.worldbank.org/indicator/SP.POP.TOTL?locations=ZJ
Xiao YF, Xiao YQ, Duan ZD (2009) The typhoon wind hazard analysis in Hong Kong of China with the new formula for Holland B parameter and the CE wind field model. The Seventh Asia-Pacific Conference on Wind Engineering, 8–12 Nov., Taipei, Taiwan
Yu Z, Wang Y, Xu H, Davidson N, Chen Y, Chen Y, Yu H (2017) On the relationship between intensity and rainfall distribution in tropical cyclones making landfall over China. J Appl Meteorol Climatol 56(10):2883–2901
Yumul GP, Servando NT, Suerte LO, Magarzo MY, Juguan LV, Dimalanta CB (2012) Tropical cyclone-southwest monsoon interaction and the 2008 floods and landslides in Panay island, central Philippines: meteorological and geological factors. Nat Hazards 62(3):827–840
Zhai AR, Jiang JH (2014) Dependence of us hurricane economic loss on maximum wind speed and storm size. Environmental Research Letters 9(6):064019